



Published in final edited form as:

*Circulation*. 2018 September 18; 138(12): 1224–1235. doi:10.1161/CIRCULATIONAHA.118.035420.

## Genetic Regulation of Fibroblast Activation and Proliferation in Cardiac Fibrosis

Shuin Park, BS<sup>\*,1,2,3</sup>, Sara Ranjbarvaziri, PhD<sup>\*,1,2,3</sup>, Fides D. Lay, PhD<sup>2,4</sup>, Peng Zhao, MD, PhD<sup>1,2</sup>, Mark J. Miller, BA<sup>1,2</sup>, Jasmeet S. Dhaliwal<sup>1,2</sup>, Adriana Huertas-Vazquez, PhD<sup>1</sup>, Xiuju Wu, MD, PhD<sup>1</sup>, Rong Qiao, MD<sup>1,2</sup>, Justin M. Soffer, BS<sup>1,2</sup>, Hanna K.A. Mikkola, MD, PhD<sup>2,4,6</sup>, Aldons J. Lusis, PhD<sup>1,5,6,7</sup>, and Reza Ardehali, MD, PhD<sup>1,2,3,6,#</sup>

<sup>1</sup>Division of Cardiology, Department of Medicine, David Geffen School of Medicine, University of California, Los Angeles, CA

<sup>2</sup>Eli and Edythe Broad Center of Regenerative Medicine and Stem Cell Research, University of California, Los Angeles, CA

<sup>3</sup>Molecular, Cellular, and Integrative Physiology Graduate Program, University of California, Los Angeles, CA

<sup>4</sup>Department of Molecular, Cell, and Developmental Biology, University of California, Los Angeles, CA

<sup>5</sup>Department of Microbiology, Immunology and Molecular Genetics, University of California, Los Angeles, CA

<sup>6</sup>Molecular Biology Institute, University of California, Los Angeles, CA

<sup>7</sup>Department of Human Genetics, University of California, Los Angeles, CA

### Abstract

**Background**—Genetic diversity and the heterogeneous nature of cardiac fibroblasts (CFBs) have hindered characterization of the molecular mechanisms that regulate cardiac fibrosis. The Hybrid Mouse Diversity Panel (HMDP) offers a valuable tool to examine genetically diverse cardiac fibroblasts and their role in fibrosis.

**Methods**—Three strains of mice (C57BL/6J, C3H/HeJ, and KK/HIJ) were selected from the HMDP and treated with either isoproterenol (ISO) or saline by an intraperitoneally implanted osmotic pump. After 21 days, cardiac function and levels of fibrosis were measured by echocardiography and trichrome staining, respectively. Activation and proliferation of CFBs were measured by *in vitro* and *in vivo* assays under normal and injury conditions. RNA-sequencing was done on isolated CFBs from each strain and results were analyzed by Ingenuity Pathway Analysis (IPA) and validated by reverse transcription-qPCR, immunohistochemistry, and ELISA.

#corresponding author: Reza Ardehali MD, PhD, Division of Cardiology, Department of Internal Medicine, David Geffen School of Medicine, University of California, Los Angeles, Los Angeles, CA 90095 USA, Phone: 310-825-2554, Fax: 310-206-5777, [ardehali@mednet.ucla.edu](mailto:ardehali@mednet.ucla.edu).

\*These authors contributed equally to this article.

### DISCLOSURES

None

**Results**—ISO treatment in C57BL/6J, C3H/HeJ, and KK/HIJ mice resulted in minimal, moderate, and extensive levels of fibrosis, respectively (n = 7–8 hearts/condition). Isolated CFbs treated with ISO exhibited strain-specific increases in the levels of activation but showed comparable levels of proliferation. Similar results were found *in vivo*, with fibroblast activation, and not proliferation, correlating with the differential levels of cardiac fibrosis after ISO treatment. RNA-sequencing revealed that CFbs from each strain exhibit unique gene expression changes in response to ISO. We identified *Ltbp2* as a commonly upregulated gene after ISO treatment. Expression of LTBP2 was elevated and specifically localized in the fibrotic regions of the myocardium after injury in mice and in human heart failure patients.

**Conclusions**—This study highlights the importance of genetic variation in cardiac fibrosis by using multiple inbred mouse strains to characterize CFbs and their response to ISO treatment. Our data suggest that, while fibroblast activation is a response that parallels the extent of scar formation, proliferation may not necessarily correlate with levels of fibrosis. Additionally, by comparing CFbs from multiple strains, we identified pathways as potential therapeutic targets and LTBP2 as a marker for fibrosis, with relevance to patients with underlying myocardial fibrosis.

### Keywords

cardiac fibroblasts; Hybrid Mouse Diversity Panel; isoproterenol; fibrosis

---

## INTRODUCTION

Acute myocardial injury or elevated pressure in the heart results in a multitude of cardiac pathologies, particularly cardiac fibrosis. It has been reported that such injury leads to activation and proliferation of cardiac fibroblasts (CFbs), some of which deposit excessive extracellular matrix (ECM) components that compromise myocardial structure and function<sup>1, 2</sup>. Despite the significant role that CFbs play in injury response, characterization of this cell type has been challenging due to their heterogeneous nature and lack of fibroblast-specific markers<sup>2, 3</sup>. Furthermore, detailed knowledge of the molecular mechanisms that regulate their specific contributions to scar development is lacking.

The Hybrid Mouse Diversity Panel (HMDP) is a collection of over 100 genotyped inbred strains of mice that allow for identification of genetic factors that contribute to various common disease traits<sup>4</sup>. In a comprehensive study by Rau et al., mice within the HMDP were phenotypically characterized following chronic treatment with isoproterenol (ISO), a  $\beta$ -adrenergic agonist<sup>5</sup>. Excessive stimulation of  $\beta$ -adrenergic receptors in the heart has been linked to increased CFb proliferation and collagen synthesis<sup>5</sup>. Chronic treatment of the HMDP with ISO resulted in a wide range of severity in cardiac hypertrophy and associated fibrosis across the different strains. These findings support the hypothesis that genetic variation influences the development and progression of cardiac dysfunction and pathological fibrosis. However, these studies evaluated changes at the cardiac tissue level and did not delineate the roles of specific cell types to each strain's respective phenotype.

In the present study, we utilized three HMDP strains with varying responses to ISO treatment to investigate the mechanisms by which their respective CFbs may regulate the process of cardiac fibrosis. We demonstrated that CFbs respond to ISO in a strain-specific

manner both *in vitro* and *in vivo*. Notably, CFbs from all three strains exhibited significant differences in levels of activation in response to ISO but had similar rates of proliferation. Additionally, we performed RNA-sequencing and identified various molecular pathways that were differentially enriched across the three strains in response to ISO. RNA-sequencing further unveiled genes that were commonly upregulated in CFbs from all three strains. Within these genes, we validated *Ltbp2* as a potential marker of fibrosis that can be applied to a genetically diverse population. Overall, our findings contribute to the understanding of cardiac fibroblast function in the context of ISO-induced cardiac fibrosis and further highlight the importance of genetic variation in complex diseases and cellular functions.

## METHODS

The data, analytic methods, and study materials will be made available to other researchers for purposes of reproducing the results or replicating the procedure. The authors declare that all supporting data are available within the article and its online supplementary files. The transcriptomics data is available under the GEO accession ID GSE109376.

### Mice

Adult female C57BL/6J, C3H/HeJ, and KK/HIJ mice (8–10 weeks) were obtained from Jackson Laboratory. All procedures were carried out with the approval of the University of California, Los Angeles (UCLA) Animal Research Committee or the Institutional Animal Care. Two operators blinded to the experimental designs performed all animal surgeries and *in vivo* analyses.

### Isoproterenol treatment

Isoproterenol (ISO) treatment was performed by implantation of Alzet osmotic pumps (Cupertino, CA) in C57B/6J, C3H/HeJ, and KK/HIJ mice (n=20). Pumps were filled with ISO (Sigma, CA) (30mg/kg body weight/per day) and implanted in the abdominal cavity under anesthesia with isoflurane. Mice were treated pre- and post-operatively with Sulfamethoxazole and Trimethoprim oral suspension (Hi-Tech Pharmacal, NY). Mice in control groups were implanted with pumps filled with saline. Mice were sacrificed and hearts were harvested 14 or 21 days post-implantation for further analysis (n=52).

### Primary cardiac fibroblast culture and characterization

Cardiac fibroblast isolation was prepared as described in the Supplementary Methods (Supplementary Table I). After sorting (BD FACSAria II), Thy1<sup>+</sup>/CD45<sup>-</sup>/Ter119<sup>-</sup>/CD11b<sup>-</sup>/CD31<sup>-</sup> cardiac fibroblasts (hereafter referred to as Thy1<sup>+</sup>HE<sup>-</sup> CFbs) were cultured on 0.1% gelatin-coated 12-well plates in DMEM supplemented with 15% FBS and antibiotics (5×10<sup>4</sup> cells/well). Media was changed 24 hours after the primary culture, followed by changes every 48 hours. Cells were passaged upon 80% confluency. After the first passage, cells were washed and cultured in serum-free culture medium supplemented with 0.5 mg/mL insulin and 0.5 mg/mL transferrin. At confluence, cells were treated with 100µm/L ISO (Sigma) or 50ng/mL TGFβ (Cell Signaling). After 72 hours, cells were washed, fixed in 4% paraformaldehyde, and stained for analysis. Cell counts were performed on ImageJ using the 'Cell Counter' plug-in by two people blind to the conditions.

### Inhibition of *in vitro* cell proliferation

Cells were isolated, expanded, and passaged upon 80% confluency with serum-free culture media ( $2.5 \times 10^4$  cells/well). Prior to treatment with ISO, cells were treated with mitomycin-C ( $10 \mu\text{g/mL}$ ) (Acros Organics) for 2 hours or irradiated for 2 minutes at 3 Gy.

### RNA-sequencing

Thy1<sup>+</sup>HE<sup>-</sup> CFbs were isolated from saline and ISO-treated hearts 14 or 21 days after pump implantation ( $n=2$  per strain/condition), and then sorted directly into TRIzol® LS Reagent (Ambion). Total RNA was extracted using the RNeasy miniElute Cleanup Kit (Qiagen), according to manufacturer's instructions. Complementary DNA (cDNA) libraries were generated using reagents provided in the KAPA mRNA Hyperprep kit. The amplified cDNA library was sequenced on an Illumina HiSeq 3000 according to manufacturer's instructions. Libraries were sequenced using 50 single-end read protocol, which yielded approximately 20 million raw reads per sample. Read quality was assessed using FastQC and reads were subsequently trimmed 5bp from the start of the reads up and 2 bp from the end of the reads. Alignment to the mm10 mouse genome were performed using STAR v2.5.3a with --twopassMode Basic option. Gene counts were generated using --quantMode GeneCounts option. Raw gene counts were transformed to counts per million (CPM) and log<sub>2</sub>-counts per million (log<sub>2</sub>-CPM) data matrix and further normalized by trimmed mean of M-values (TMM) method in the edgeR Bioconductor package. Genes with CPM<1 across all samples were excluded from further analysis. To determine differentially expressed genes, the *voom* method of *limma* was applied, accommodating the mean-variance in the linear model using precision weight, and significant gene set was selected with nominal p-value<0.05 threshold. Global functional analyses, network analyses, and canonical pathway analyses were performed using Ingenuity Pathway Analysis (Ingenuity® Systems, [www.ingenuity.com](http://www.ingenuity.com)).

### Statistical analysis

Statistical testing was performed with GraphPad Prism 6. Results are presented as mean ± SEM and were analyzed using one-way ANOVA, two-way ANOVA or Student t-test (significance was assigned for P<0.05). Multiple comparisons were considered by Tukey's multiple comparison test, the Sidak method, or the Holm-Sidak method.

## RESULTS

### Pathological analysis of ISO-induced cardiac function and fibrosis in selected mouse strains

The entire HMDP was characterized at baseline and in response to ISO treatment to determine the extent of cardiac fibrosis (Figure 1A). The survey revealed significant variations in cardiac pathophysiology and fibrosis under baseline conditions and in response to ISO administration<sup>5, 6</sup>. Based on this considerable variability, we selected three representative strains that exhibited distinct pathological phenotypes: C57BL/6J, C3H/HeJ, and KK/HIJ, showing minimal, moderate, and substantial myocardial fibrosis after ISO injury, respectively. Adult female mice (8–10 weeks, 20–28 grams) from each strain were intraperitoneally implanted with an Alzet micro-osmotic pump containing saline or ISO.

Mice from all strains were of similar size (Supplementary Figure IA) and body weight (data not shown). Throughout the course of treatment, the mice did not display adverse physical symptoms in response to ISO. After 21 days of treatment, animals were sacrificed and hearts were harvested for analysis. Masson's trichrome staining demonstrated minimal to no visible fibrotic areas in all mice treated with saline (Figure 1B). After ISO treatment, both C3H/HeJ and KK/HIJ hearts exhibited clear fibrotic areas (blue), while C57BL/6J hearts had minimal amounts of fibrosis. Consistent with the histological observations, quantitative analysis of the fibrotic areas showed significant differences across the selected strains, with KK/HIJ hearts consistently exhibiting the greatest area of fibrosis in response to ISO (C57BL/6J: Saline=0.1±0.1% ISO=1.2±0.1%, C3H/HeJ: Saline=0.3±0.1% ISO=2.4±0.4%, KK/HIJ: Saline=0.3±0.1% ISO=6.4±0.7%) (Figure 1C). Additionally, ISO treatment caused observable increases in heart size (Supplementary Figure IB) and heart weight/tibia length ratios (Supplementary Figure IC) in both KK/HIJ and C3H/HeJ strains, while C57BL/6J mice showed minimal signs of cardiac hypertrophy.

Functional echocardiography analysis demonstrated increased left ventricle end-diastolic dimension (EDD) and end-systolic dimension (ESD) in the C3H/HeJ and KK/HIJ strains 21 days after ISO treatment (Supplementary Figure ID). Furthermore, these strains exhibited significant decreases in ejection fraction (C57BL/6J: Saline=+1.2±2.3% ISO=+0.15±3.13%, C3H/HeJ: Saline=+2.0±5.0% ISO=-15.9±5.2%, KK/HIJ: Saline=+2.2±3.2% ISO=-17.9±6.6%) (Figure 1D) and fractional shortening (Supplementary Figure IE) after ISO treatment. In contrast, C57BL/6J mice had preserved cardiac function in ISO-treated compared to saline-treated hearts (Figure 1D and Supplementary Figure IE).

These results confirm that chronic  $\beta$ -adrenergic stimulation in different mouse strains leads to varying severity of cardiac fibrosis. These phenotypical differences were used to further characterize the contributions of CFbs to ISO-induced fibrosis.

### ***In vitro* characterization of strain-specific cardiac fibroblasts in response to ISO**

Based on the varying levels of fibrosis exhibited by the three selected strains, we focused on characterizing strain-specific CFbs and their potential role in generating the observed patterns of cardiac fibrosis. Initially, CFbs from each strain were isolated and cultured as described in the Supplemental Methods<sup>2</sup>. While our isolation protocol does not purify the entire CFb population, it ensures that the same population of cells will be compared across the three strains. Phase contrast images and immunocytochemistry (ICC) confirmed that CFbs from all strains exhibit similar mesenchymal morphology (Supplementary Figure IIA) and express fibroblast markers collagen 1 (Col1) and PDGFR $\alpha$  (Supplementary Figure IIB and IIC). We then sought to determine whether these fibroblasts exhibited similar patterns of activation and proliferation in culture. CFbs were stained for the expression of  $\alpha$ -smooth muscle actin ( $\alpha$ SMA), a marker associated with activated fibroblasts<sup>7</sup>, and Phospho-Histone H3 (pHH3)<sup>8</sup>, for proliferation analysis. We observed very low expression of  $\alpha$ SMA within Col1<sup>+</sup> CFbs from all strains (Supplementary Figure IID and IIE), indicating that these cells do not become activated without stimuli, and have similar rates of proliferation (%pHH3<sup>+</sup> nuclei) at the basal level (Supplementary Figure IIF and IIG).

We next examined whether strain-specific CFbs may have differential responses to ISO *in vitro*. CFbs from each strain were isolated, expanded, and passaged prior to being treated with culture media containing ISO (Figure 2A). Cells were then fixed and characterized by phase contrast microscopy (Figure 2B) and ICC. A significant percentage of CFbs from C3H/HeJ and KK/HIJ began to co-express  $\alpha$ SMA and Col1, while CFbs from C57BL/6J exhibited minimal  $\alpha$ SMA expression in the presence of ISO (C57BL/6J: No ISO=0.8±0.5% ISO=1.9±1.8%, C3H/HeJ: No ISO=1.0±0.5% ISO=12.3±1.7%, KK/HIJ: No ISO=1.1±0.5% ISO=7.5±1.6%) (Figure 2C and 2D). Immunostaining for pHH3 revealed that the rate of proliferation was significantly increased across all three strains to similar levels when compared to their respective untreated control groups (C57BL/6J: No ISO=5.6±1.2% ISO=20.9±3.5%, C3H/HeJ: No ISO=4.9±1.4% ISO=16.9±4.8%, KK/HIJ: No ISO=3.4±1.4% ISO=20.0±2.9%) (Figure 2E and 2F). CFbs isolated from mice pre-treated with implanted ISO osmotic pumps (Supplementary Figure IIIA) did not exhibit significant changes in activation or proliferation in response to additional *in vitro* ISO treatment (Supplementary Figure IIIB and IIIC). This may be attributed to an already stimulated state of cells before culture, resulting in minimal response to ISO *in vitro*<sup>9</sup>.

We additionally treated CFbs *in vitro* with TGF $\beta$ , a pro-fibrotic cytokine, for 72 hours (Supplementary Figure IVA)<sup>10</sup>. The morphology of the cells appeared grossly similar across all three strains (Supplementary Figure IVB). CFbs from all three strains exhibited significant increases in the level of activation from baseline, although the levels in KK/HIJ were significantly higher than in C57BL/6J (Supplementary Figure IVC and IVD). The proliferation rates of CFbs from all strains increased similarly in response to TGF $\beta$  (Supplementary Figure IVE).

Together, these data suggest that cultured CFbs respond to ISO in a strain-specific manner. While ISO treatment resulted in differing levels of activation in cultured CFbs, their levels of proliferation were similar.

### Cardiac fibroblasts demonstrate strain-specific responses to ISO treatment *in vivo*

While other studies have viewed fibroblast activation and proliferation to be interdependent responses to stimulation, our *in vitro* results suggest otherwise. To determine whether a similar behavior is observed *in vivo*, we investigated CFb activation and proliferation after ISO stimulation in the three selected strains.

First, we observed the presence of activated fibroblasts in C57BL/6J, C3H/HeJ, and KK/HIJ mice in response to ISO treatment. Immunohistochemistry (IHC) was used to observe co-localization of Col1 with  $\alpha$ SMA or periostin for the identification of activated CFbs<sup>11, 12</sup>. In all saline-treated groups, Col1 staining was mainly present around larger vessels and co-localization with  $\alpha$ SMA was exceedingly rare (Figure 3A). However, after ISO treatment, there was an increase in Col1 staining, particularly in C3H/HeJ and KK/HIJ hearts (Supplementary Figure VA). Many Col1<sup>+</sup> cells co-expressed  $\alpha$ SMA in both perivascular and interstitial regions of the myocardium in C3H/HeJ and KK/HIJ hearts, indicating the presence of activated CFbs (Figure 3A). This increase was quantified as the area of Col1<sup>+</sup> $\alpha$ SMA<sup>+</sup> staining normalized to the total area of each heart section (C57BL/6J: Saline=0.5±0.2 ISO=5.2±1.0, C3H/HeJ: Saline=2.2±0.6 ISO=12.4±2.2, KK/HIJ:

Saline=4.8±1.5 ISO=42.0±4.7) (Figure 3B). IHC for periostin also confirmed the differential levels of activated CFbs observed across the three strains (Supplementary Figure VB). Consistent with our *in vitro* results, the levels of CFb activation corresponded with the amount of fibrosis seen within each strain.

Next, we sought to assess the proliferative behavior of CFbs *in vivo* after ISO injury. Mice were injected with Bromodeoxyuridine (BrdU) at the time of micro-osmotic pump implantation for saline/ISO and exposed to BrdU diluted in drinking water throughout the 21 days of treatment (Figure 3C). IHC of the control hearts demonstrated low levels of BrdU<sup>+</sup> proliferating CFbs throughout the myocardium. However, with ISO treatment, we observed a significantly higher number of BrdU<sup>+</sup> cells throughout the perivascular and interstitial Col1<sup>+</sup> regions in all three strains (Figure 3D). Flow cytometry demonstrated similar percentages of BrdU<sup>+</sup> CFbs in the control groups for all three strains. The proportion of BrdU<sup>+</sup> CFbs significantly increased to a similar amount after ISO treatment in all three strains (C57BL/6J: Saline=5.8±1.5% ISO=20.9±0.6%, C3H/HeJ: Saline=7.1±0.8% ISO=32.7±5.3%, KK/HIJ: Saline=6.2±0.8% ISO=23.4±1.4%) (Figure 3E and Supplementary Figure VC).

These results demonstrate that while a similar pattern of CFb proliferation was observed in all three strains after ISO treatment, the extent of cardiac fibrosis directly correlated with the number of activated CFbs.

### **Inhibition of cardiac fibroblast proliferation *in vitro* does not affect their activation levels**

Our results suggest that CFb proliferation and activation may be distinct responses to ISO treatment with different phenotypic presentation depending on genetic background. To confirm this, we sought to inhibit CFb proliferation *in vitro* and determine whether it would affect the activation of these cells.

CFbs from each strain were isolated, cultured, and subjected to one of three conditions: (i) culture in normal media, (ii) treatment with mitomycin-C (mito-C) for 2 hours, or (iii) irradiation (IR) for 2 minutes. We chose treatment with mito-C or irradiation as two independent methods to inhibit CFb proliferation<sup>13</sup>. We then exposed the cells to ISO and conducted ICC for pHH3 and  $\alpha$ SMA (Figure 4A). In all three strains, the percentages of pHH3<sup>+</sup> nuclei were significantly reduced following mito-C and IR treatment (C57BL/6J: Control=17.38±6.1% Mito-C=0.5±0.3% IR=3.5±1.3%, C3H/HeJ: Control=11.69±1.5% Mito-C=2.2±0.9% IR=3.7±1.6%, KK/HIJ: Control=14.8±0.5% Mito-C=0.3±0.3% IR=2.7±1.8%) (Figure 4B). However, we did not observe significant differences in the percentage of CFbs that expressed markers for CFb activation such as  $\alpha$ SMA (C57BL/6J: Control=0.2±0.1% Mito-C=0.1±0.1% IR=1.5±0.7%, C3H/HeJ: Control=5.0±0.7% Mito-C=4.1±1.6% IR=2.5±0.8%, KK/HIJ: Control=18.5±8.5% Mito-C=13.11±2.06%, IR=8.1±0.7%) (Figure 4C). These results confirm that CFb proliferation and activation do not necessarily correlate with each other and may contribute to fibrosis in unique manners.

## Strain-specific cardiac fibroblasts have unique transcriptional profiles in response to *in vivo* ISO treatment

The use of multiple genetic strains for transcriptome analysis allows for a comprehensive approach to determine potential genetic contributors of specific phenotypes. To further characterize CFbs within the three selected strains, we performed RNA-sequencing on isolated CFbs from C57BL/6J, C3H/HeJ, and KK/HIJ mice that underwent saline or ISO treatment for 21 days. The effects of ISO on each strain's transcriptome was unique, as seen by the global heatmap of differential gene expression of all three strains, further justifying the need to study strain-specific phenotypes (Figure 5A). Based on the *in vitro* and *in vivo* results, we focused on genes mainly associated with fibrosis and proliferation. We observed that genes related to fibroblast activation and fibrosis were highly upregulated in KK/HIJ CFbs in response to ISO compared to C3H/HeJ and C57BL/6J CFbs (Figure 5B). In contrast, we observed comparable expression levels of select cell cycle and proliferation genes across the three strains (Figure 5C).

Furthermore, we used Ingenuity Pathway Analysis (IPA) to identify enriched pathways which may be involved in regulating such differences within each strain (Supplementary Figure VIA). Overall, C3H/HeJ and KK/HIJ CFbs exhibited higher activation scores for several pro-fibrotic pathways when compared to C57BL/6J, such as the TGF $\beta$  signaling<sup>14</sup>,  $\beta$ -adrenergic signaling<sup>5</sup>, and Endothelin-1 signaling pathways<sup>15</sup> (Supplementary Figure VIB). The GP6 signaling pathway was of particular interest as it showed the highest activation scores in KK/HIJ CFbs and was one of the more significantly enriched pathways identified by IPA (Supplementary Figure VIA and VIB).

To identify changes that occurred throughout the course of injury, we additionally isolated CFbs from ISO-treated mice 14 days after pump implantation for RNA-sequencing. Compared to saline-treated groups, CFbs from all strains exhibited an extensive number of differentially expressed genes (Supplementary Figure VIIA) and enriched pathways (Supplementary Figure VIIB) between days 14 and 21 of injury, suggesting that changes continue to occur at the transcriptome level in CFbs up until the final week of treatment. Between days 14 and 21, C57BL/6J CFbs exhibited negative activation scores of various pro-fibrotic pathways (Supplementary Figure VIIC). On the other hand, C3H/HeJ CFbs exhibited higher levels of activation of several pro-fibrotic pathways, suggesting that CFbs are continuing to respond to ISO treatment (Supplementary Figure VIIC). Finally, KK/HIJ CFbs did not exhibit significant changes in pathway activation between 14 and 21 days of treatment. (Supplementary Figure VIIC). According to our IPA analysis, each strain demonstrated distinct differences in pathway activation at different time points of ISO treatment. Further exploration of these pathways is required to delineate the mechanisms by which they alter ISO-induced cardiac fibrosis.

### ***Ltbp2* is upregulated in response to cardiac fibrosis**

Like genome-wide association studies (GWAS), the HMDP facilitates identification of unique genes that may be associated with complex phenotypic traits. To account for diversity seen in heart failure pathologies, we sought to identify genes that can be associated with fibrosis regardless of genetic background. From the RNA-sequencing data, we focused on



genes that were upregulated within each strain in response to ISO. Several of these genes overlapped across two strains, but the majority of the genes were unique to each strain (Figure 6A). We focused on genes that were upregulated in all three strains in response to ISO and identified *Ltbp2* to be of interest (Figure 6B and Supplementary Figure VIIIA). Reverse transcription-qPCR (RT-qPCR) for *Ltbp2* within CFbs confirmed the trends seen within the RNA-sequencing data (C57BL/6J:  $2.0 \pm 0.5$ , C3H/HeJ:  $3.6 \pm 0.7$ , KK/HIJ:  $3.2 \pm 0.8$ ) (Figure 6C and Supplementary Table II).

To confirm the presence of LTBP2 protein in fibrosis, we conducted IHC on cardiac sections from all three strains after ISO treatment. In saline-treated hearts, there was minimal expression of LTBP2 throughout the myocardium (Figure 6D). However, in response to ISO, LTBP2 co-localized with DDR2, a marker for fibroblasts, and  $\alpha$ SMA (Figure 6D). The expression of LTBP2 was specifically localized to the fibrotic regions, even in C57BL/6J hearts, where there was minimal fibrosis (Figure 6D). As it is a secreted protein, we additionally sought to determine whether ISO treatment elevates LTBP2 levels in circulation. We found that LTBP2 levels were significantly increased in plasma of KK/HIJ mice, with upward trends in C57BL/6J and C3H/HeJ mice, after ISO treatment (Supplementary Figure VIIIB and Supplementary Table III).

To determine whether LTBP2 expression is also present in other models of fibrosis, we performed transverse aortic constriction (TAC) surgery on the three mouse strains<sup>16</sup>. We observed cardiac hypertrophy and the presence of myocardial fibrosis in the three strains after TAC (data not shown). In C57BL/6J mice, RNA-sequencing and RT-qPCR demonstrated significant increases in *Ltbp2* expression in CFbs 7 days after TAC surgery compared to sham (Supplementary Figure VIIC and VIID). Additionally, IHC showed that LTBP2 was preferentially localized in the fibrotic areas within the myocardium of mice that underwent TAC (Figure 6D).

Finally, we investigated whether LTBP2 is upregulated in human plasma with underlying heart failure. We found that average LTBP2 levels were mildly increased in patients with heart failure with reduced ejection fraction (HFrEF) when compared to healthy individuals. (Supplementary Figure IXA and Supplementary Table IV). Furthermore, IHC staining of human myocardial tissue from heart failure patients revealed LTBP2 expression to be significantly increased compared to expression in the healthy human myocardium (Supplementary Figure IXB).

Taken together, our results suggest that the expression of LTBP2 may be indicative of the development of cardiac fibrosis, but its specific role in fibrosis requires further exploration.

## DISCUSSION

Despite the functional significance of CFbs in cardiovascular disease, the specific contributions of these cells to cardiac fibrosis are not completely understood. Previous studies revealed a wide spectrum of cardiac pathology across various inbred strains of mice when subjected to chronic  $\beta$ -adrenergic stimulation by ISO<sup>5, 6</sup>. We hypothesized that characterizing fibroblasts of multiple strains with different severities of ISO-induced cardiac

fibrosis would allow us to dissect the contributions of these cells to scar development. Our results show that fibroblast activation, not proliferation, correlates with the striking differences in fibrosis among the divergent strains. Moreover, comparisons of gene expression profiles across the strains revealed differences in underlying mechanistic pathways and led to the identification of a potential marker of fibrosis.

While recent research has focused on how CFbs become activated and proliferate in response to injury<sup>17</sup>, the mechanisms by which these processes dictate scar development have yet to be elucidated. Prior to this study, CFb activation and proliferation were generally considered to be interconnected responses that contribute to fibrosis<sup>17, 18</sup>. Here, by comparing CFbs from three selected strains of the HMDP – C57BL/6J, C3H/HeJ, and KK/HIJ – we discovered that there is a direct correlation of CFb activation with the severity of fibrosis, while CFbs from all strains exhibited similar proliferative capacity in response to ISO. These results suggest that CFb proliferation may be an independent response from CFb activation and that levels of proliferation do not necessarily correlate with the extent of scar formation. It is possible that CFb proliferation is an indicator of CFb stimulation, but the functional roles of this phenomenon require further studies.

Myocardial injury evokes multiple signaling pathways in cardiac fibroblasts that ultimately lead to the activation of genes that regulate cardiac fibrosis<sup>19</sup>. To delineate gene expression differences between CFbs from each select strain, we conducted RNA-sequencing on sorted CFbs after saline and ISO treatment. After ISO treatment, CFbs from each strain responded with distinct changes in their gene expression profiles. Our results revealed many genes with small fold changes and the analysis was conducted to be inclusive of these changes. We observed enrichment of fibroblast activation genes that paralleled the extent of fibrosis observed in each strain, while the upregulation of proliferation genes was comparable across all strains. IPA analysis identified the GP6 signaling pathway as exhibiting activation scores that corresponded with the levels of fibrosis seen across the three selected strains. GP6 is a collagen receptor abundantly expressed on platelets that activates a downstream signaling cascade promoting platelet aggregation and thrombus formation<sup>20</sup>. The role of this signaling pathway in fibroblasts has yet to be explored, but our results suggest that modulation of this signaling cascade may regulate the formation of fibrosis. Our RNA-sequencing data also revealed that genetic differences may influence the timely progression of scar formation. In C57BL/6J mice, CFbs were not immune to ISO treatment, but rather exhibited a downregulation of pro-fibrotic pathways between day 14 and day 21 of treatment. On the contrary, C3H/HeJ mice appeared to display a slow progression towards the formation of fibrosis, evidenced by the continuing changes in gene expression profiles between day 14 and day 21. Finally, KK/HIJ mice, as the most sensitive strain, exhibited surprisingly few changes in canonical pathway activation between day 14 and day 21 of treatment, suggesting that CFbs may have already undergone transcriptional changes in response to ISO prior to the time of analysis. Ultimately, these findings raise questions regarding whether phenotypic and/or transcriptomic changes observed after cardiac injury within a single mouse strain can be applicable to other strains. It is important to interrogate these pathways to gain insight into mechanisms of CFb activation, explore how cardiac fibrosis is regulated, and perhaps design novel anti-fibrotic therapies.

Heart failure resulting from prolonged interstitial fibrosis is a highly heterogeneous disorder influenced by many environmental and genetic factors. GWAS allows for the identification of genetic variations on complex traits such as heart failure<sup>21</sup>. However, multiple large-scale GWAS studies have provided limited success in identifying genetic signals driving heart failure<sup>22</sup>. This is partly due to the paucity of quantitative phenotypic data as well as diverse environmental factors. Therefore, there have been challenges in developing treatments for heart failure and cardiac fibrosis that are applicable to a diverse population. The HMDP is a unique tool to mimic in mice the genetic variance and substantial diversity of heart failure development seen in humans. While previous studies have sought to identify genetic markers uniquely associated with heart failure in a specific genetic background, we sought to investigate common markers that are associated with cardiac fibrosis in a panel of genetically diverse mouse strains. Our results revealed *Ltbp2* to be upregulated in CFbs from all three strains and that the expression of LTBP2 was primarily localized in the fibrotic regions. LTBP2 is part of the Latent TGF $\beta$ 1-Binding Protein family, which have been shown to participate in the regulation of TGF $\beta$  signaling and display high affinity binding sites for extracellular matrix proteins. However, while the functions of LTBP1<sup>23</sup>, LTBP3<sup>24</sup>, and LTBP4<sup>25</sup> in disease have been extensively characterized, the role of LTBP2 in cardiac injury is still unclear. Whether LTBP2 is merely a surrogate for cardiac fibrosis or is involved in its pathogenesis is not entirely known. Furthermore, the specificity of LTBP2 to cardiac fibrosis, and its potential role in the manifestation of other types of organ fibrosis cannot be disregarded. However, our results in both mice and human heart failure patients support the possibility of LTBP2 being used as a marker for fibrosis that can be used across a genetically diverse population.

Our data demonstrates the importance of considering genetic backgrounds when conducting studies on CFbs that reflect changes in cardiac phenotype in response to injury. The comparisons conducted across multiple strains allowed for a unique approach in associating CFbs with a spectrum of ISO-induced fibrosis, rather than just the presence of fibrosis itself. This form of analysis allowed us to determine significant factors that directly correlate with the development of scar tissue, which may have not been recognized if the study was done within a single strain. This multiple-strain approach, when combined with molecular and cell-based characterizations, serves as an important tool for future work delineating the functions not only of CFbs, but also of a variety of cardiac cell types.

## Supplementary Material

Refer to Web version on PubMed Central for supplementary material.

## Acknowledgments

S.R., S.P., and R.A. conceived the project and designed the experiments. X.W. and A. J. L. assisted with the initial design. S.P. and S.R. performed all experiments, analyzed data and prepared the figures. S.P. and S.R. had full access to all the data in the study and take responsibility for the integrity of the data and the accuracy of the data analysis. S.P., S.R., and R.A. wrote the manuscript. H.K.A.M. and F.D. L. helped with the analysis of RNA-sequencing data and acknowledge support the Quantitative and Computational Biosciences Community directed by Matteo Pellegrini. A.H-V. assisted with obtaining human serum samples. M.J.M., J.S.D., R.Q., and J.M.S. assisted with all stainings. P.Z. performed all surgeries. All authors reviewed the manuscript. Echocardiograms were performed in Dr. Yibin Wang's lab. We would like to acknowledge Shuxun Ren with his assistance in the initial surgeries. The LTBP2 antibody was a generous gift from Dr. Marko Hyytiäinen from the University of Helsinki,

Finland. We are grateful for the expert technical assistance from the UCLA Broad Stem Cell Research Center Flow Cytometry Core, Confocal Microscopy Core, and Clinical Microarray Core. We acknowledge Ngoc B. Nguyen and James L. Engel for their critical reading of this article.

#### SOURCES OF FUNDING

This work was supported by the NIH DP2 HL127728 (R.A.); UCLA Broad Stem Cell Research Center-Rose Hills Foundation Research Award (R.A.); the Eli & Edythe Broad Center of Regenerative Medicine and Stem Cell Research Center at UCLA Research Award (R.A. and H.K.A.M.); NIH HL28481 (A.H-V., X.W., and A.J.L.); NIH HL123295 (A.H-V., X.W., and A.J.L.); and the American Heart Association 14GRNT20480340 and 16IRG27260285 (H.K.A.M.). S.P. was supported by the Ruth L. Kirschstein National Research Service Award T32HL69766. S. R. was supported by the UCLA Graduate Programs in Bioscience. F. D. L. was supported by the UCLA Quantitative and Computational Biosciences Collaboratory Post-Doctoral Fellowship.

#### References

1. Fan D, Takawale A, Lee J, Kassiri Z. Cardiac fibroblasts, fibrosis and extracellular matrix remodeling in heart disease. *Fibrogenesis Tissue Repair*. 2012; 5:15.doi: 10.1186/1755-1536-5-15 [PubMed: 22943504]
2. Ali SR, Ranjbarvaziri S, Talkhabi M, Zhao P, Subat A, Hojjat A, Kamran P, Muller AM, Volz KS, Tang Z, Red-Horse K, Ardehali R. Developmental heterogeneity of cardiac fibroblasts does not predict pathological proliferation and activation. *Circ Res*. 2014; 115:625–635. DOI: 10.1161/CIRCRESAHA.115.303794 [PubMed: 25037571]
3. Travers JG, Kamal FA, Robbins J, Yutzey KE, Blaxall BC. Cardiac Fibrosis: The Fibroblast Awakens. *Circ Res*. 2016; 118:1021–1040. DOI: 10.1161/CIRCRESAHA.115.306565 [PubMed: 26987915]
4. Lusis AJ, Seldin MM, Allayee H, Bennett BJ, Civelek M, Davis RC, Eskin E, Farber CR, Hui S, Mehrabian M, Norheim F, Pan C, Parks B, Rau CD, Smith DJ, Vallim T, Wang Y, Wang J. The Hybrid Mouse Diversity Panel: a resource for systems genetics analyses of metabolic and cardiovascular traits. *J Lipid Res*. 2016; 57:925–942. DOI: 10.1194/jlr.R066944 [PubMed: 27099397]
5. Rau CD, Wang J, Avetisyan R, Romay MC, Martin L, Ren S, Wang Y, Lusis AJ. Mapping genetic contributions to cardiac pathology induced by Beta-adrenergic stimulation in mice. *Circ Cardiovasc Genet*. 2015; 8:40–49. DOI: 10.1161/CIRCGENETICS.113.000732 [PubMed: 25480693]
6. Wang JJ, Rau C, Avetisyan R, Ren S, Romay MC, Stolin G, Gong KW, Wang Y, Lusis AJ. Genetic Dissection of Cardiac Remodeling in an Isoproterenol-Induced Heart Failure Mouse Model. *PLoS Genet*. 2016; 12:e1006038.doi: 10.1371/journal.pgen.1006038 [PubMed: 27385019]
7. Baum J, Duffy HS. Fibroblasts and myofibroblasts: what are we talking about? *J Cardiovasc Pharmacol*. 2011; 57:376–379. DOI: 10.1097/FJC.0b013e3182116e39 [PubMed: 21297493]
8. Crosio C, Fimia GM, Loury R, Kimura M, Okano Y, Zhou H, Sen S, Allis CD, Sassone-Corsi P. Mitotic phosphorylation of histone H3: spatio-temporal regulation by mammalian Aurora kinases. *Mol Cell Biol*. 2002; 22:874–885. [PubMed: 11784863]
9. Squires CE, Escobar GP, Payne JF, Leonardi RA, Goshorn DK, Sheats NJ, Mains IM, Mingoia JT, Flack EC, Lindsey ML. Altered fibroblast function following myocardial infarction. *J Mol Cell Cardiol*. 2005; 39:699–707. [PubMed: 16111700]
10. Leask A. TGFbeta, cardiac fibroblasts, and the fibrotic response. *Cardiovasc Res*. 2007; 74:207–212. [PubMed: 16919613]
11. Kanisicak O, Khalil H, Ivey MJ, Karch J, Maliken BD, Correll RN, Brody MJ, SCJL, Aronow BJ, Tallquist MD, Molkentin JD. Genetic lineage tracing defines myofibroblast origin and function in the injured heart. *Nat Commun*. 2016; 7:12260.doi: 10.1038/ncomms12260 [PubMed: 27447449]
12. Snider P, Standley KN, Wang J, Azhar M, Doetschman T, Conway SJ. Origin of cardiac fibroblasts and the role of periostin. *Circ Res*. 2009; 105:934–947. DOI: 10.1161/CIRCRESAHA.109.201400 [PubMed: 19893021]
13. Ponchio L, Duma L, Oliviero B, Gibelli N, Pedrazzoli P, Robustelli della Cuna G. Mitomycin C as an alternative to irradiation to inhibit the feeder layer growth in long-term culture assays. *Cytotherapy*. 2000; 2:281–286. [PubMed: 12042037]

14. Biernacka A, Dobaczewski M, Frangogiannis NG. TGF-beta signaling in fibrosis. *Growth Factors*. 2011; 29:196–202. DOI: 10.3109/08977194.2011.595714 [PubMed: 21740331]
15. Ross B, D’Orleans-Juste P, Giaid A. Potential role of endothelin-1 in pulmonary fibrosis: from the bench to the clinic. *Am J Respir Cell Mol Biol*. 2010; 42:16–20. DOI: 10.1165/rcmb.2009-0175TR [PubMed: 19717811]
16. deAlmeida AC, van Oort RJ, Wehrens XH. Transverse aortic constriction in mice. *J Vis Exp*. 2010; 38:1729.doi: 10.3791/1729
17. Chen W, Frangogiannis NG. Fibroblasts in post-infarction inflammation and cardiac repair. *Biochim Biophys Acta*. 2013; 1833:945–953. DOI: 10.1016/j.bbamcr.2012.08.023 [PubMed: 22982064]
18. Midgley AC, Rogers M, Hallett MB, Clayton A, Bowen T, Phillips AO, Steadman R. Transforming growth factor-beta1 (TGF-beta1)-stimulated fibroblast to myofibroblast differentiation is mediated by hyaluronan (HA)-facilitated epidermal growth factor receptor (EGFR) and CD44 co-localization in lipid rafts. *J Biol Chem*. 2013; 288:14824–14838. DOI: 10.1074/jbc.M113.451336 [PubMed: 23589287]
19. Manabe I, Shindo T, Nagai R. Gene expression in fibroblasts and fibrosis: involvement in cardiac hypertrophy. *Circ Res*. 2002; 91:1103–1113. [PubMed: 12480810]
20. Watson SP, Auger JM, McCarty OJ, Pearce AC. GPVI and integrin alphaIIb beta3 signaling in platelets. *J Thromb Haemost*. 2005; 3:1752–1762. [PubMed: 16102042]
21. Stranger BE, Stahl EA, Raj T. Progress and promise of genome-wide association studies for human complex trait genetics. *Genetics*. 2011; 187:367–383. DOI: 10.1534/genetics.110.120907 [PubMed: 21115973]
22. Rau CD, Lusic AJ, Wang Y. Genetics of common forms of heart failure: challenges and potential solutions. *Curr Opin Cardiol*. 2015; 30:222–227. DOI: 10.1097/HCO.0000000000000160 [PubMed: 25768955]
23. Dallas SL, Keene DR, Bruder SP, Saharinen J, Sakai LY, Mundy GR, Bonewald LF. Role of the latent transforming growth factor beta binding protein 1 in fibrillin-containing microfibrils in bone cells in vitro and in vivo. *J Bone Miner Res*. 2000; 15:68–81. [PubMed: 10646116]
24. Penttinen C, Saharinen J, Weikkolainen K, Hyttiainen M, Keski-Oja J. Secretion of human latent TGF-beta-binding protein-3 (LTBP-3) is dependent on co-expression of TGF-beta. *J Cell Sci*. 2002; 115:3457–3468. [PubMed: 12154076]
25. Bultmann-Mellin I, Dinger K, Debuschewitz C, Loewe KMA, Melcher Y, Plum MTW, Appel S, Rapp G, Willenborg S, Schauss AC, Jungst C, Kruger M, Dressler S, Nakamura T, Wempe F, Alejandro Alcazar MA, Sterner-Kock A. Role of LTBP-4 in alveolarization, angiogenesis and fibrosis in lungs. *Am J Physiol Lung Cell Mol Physiol*. 2017; 313:L687–L698. DOI: 10.1152/ajplung.00031.2017 [PubMed: 28684544]

## CLINICAL PERSPECTIVE

### What is new?

- This study utilizes a novel multiple-strain approach to characterize the contributions of cardiac fibroblasts to the formation of isoproterenol-induced cardiac fibrosis.
- While cardiac fibroblast activation levels correlated with the extent of fibrosis, proliferation was found to be similarly increased across all strains, suggesting that these two responses are not mutually inclusive.
- *Ltbp2* was identified as a common gene that is upregulated within all strains after treatment with isoproterenol and LTBP2 was shown to localize in areas of fibrosis in the myocardium of patients with heart failure, suggestive of its potential as a biomarker for fibrosis.

### What are the clinical implications?

- Understanding the responses of genetically diverse cardiac fibroblasts to injury will allow for the development of efficacious therapies for treating cardiac fibrosis.
- The results of this study suggest that levels of cardiac fibroblast proliferation may not be an indicative measure of the extent of cardiac fibrosis.
- The specificity of LTBP2 expression in the fibrotic regions of the myocardium suggests that it may be a potential target for reducing levels of cardiac fibrosis.

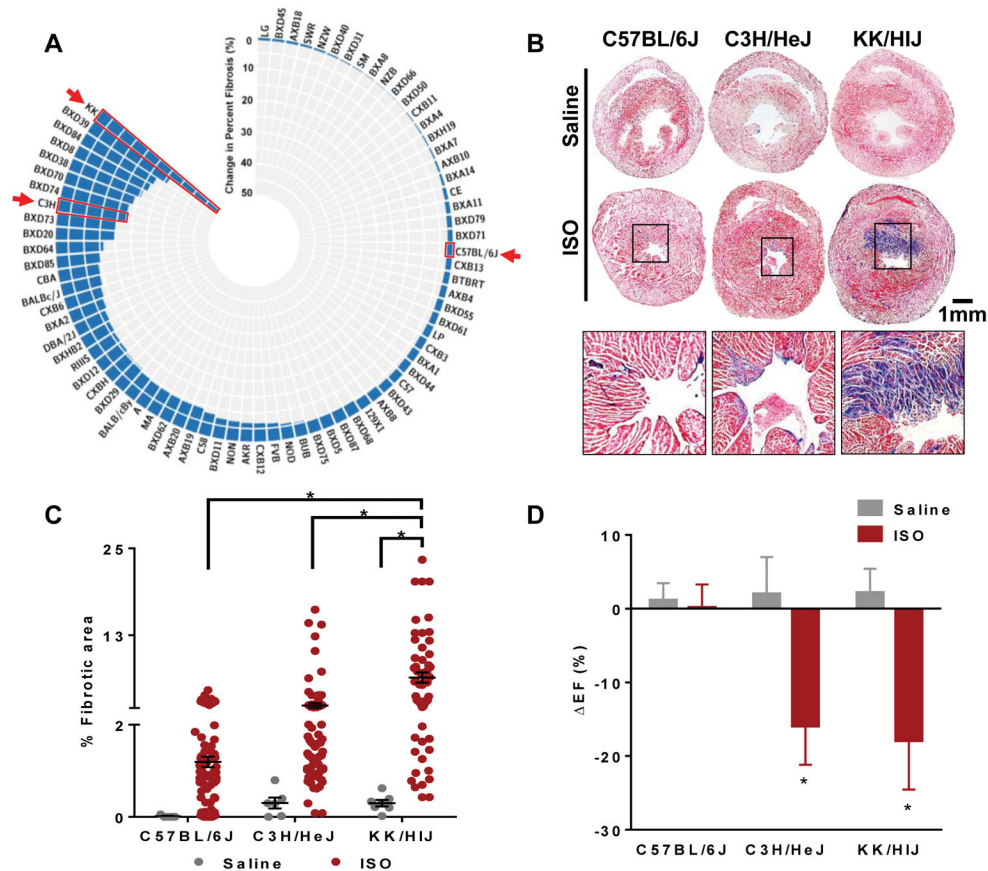


**Figure 1. Severity of fibrosis varies across different mouse strains (C57BL/6J, C3H/HeJ, KK/HIJ) in response to ISO treatment**

(A) Wide variation in percentage of fibrosis was observed between the strains of the hybrid mouse diversity panel (HMDP) after ISO treatment. (B) Masson's Trichrome stained sections of hearts from the three selected strains after 21 days of saline/ISO treatment (n=7–8 mice per condition). (C) Quantification of fibrotic area as a percentage of total section area (n=10–12 sections per heart). (D) Left ventricular ejection fractions (EF) were measured by echocardiography in both saline- and ISO-treated groups across the different strains at day 0 and day 21 of treatment. Changes in ejection fraction between these two timepoints were determined as the  $\Delta$ EF for each mouse (n=20 mice per strain). Data presented as mean  $\pm$  SEM. Two-way ANOVA, \*P < 0.05. Scale bar: 1mm

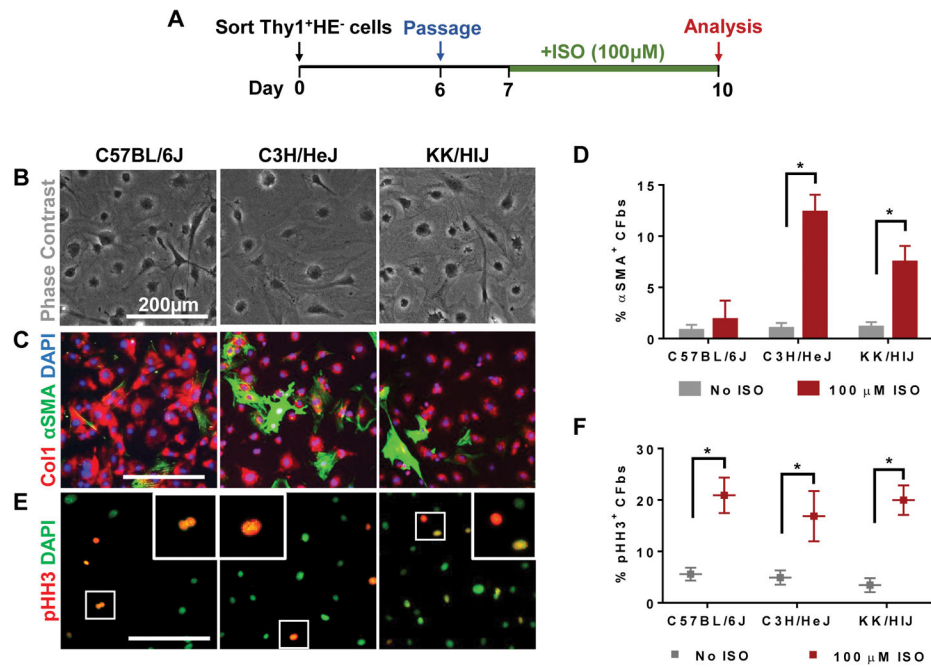


**Figure 2. *In vitro* ISO treatment affects CFb activation and proliferation in a strain-specific manner**

(A) Schematic diagram outlining the *in vitro* experiments. Cells were isolated by FACS, expanded, and passaged prior to exposure to ISO for 72 hours. (B) Phase contrast images of CFbs after ISO treatment. (C) Activated fibroblasts were identified by co-expression of Col1 (red) and  $\alpha$ SMA (green) after ISO treatment. (D) Quantification of activated CFbs (Col1<sup>+</sup> $\alpha$ SMA<sup>+</sup> cells) is shown as a percentage of double-positive cells relative to all fibroblasts (Col1<sup>+</sup> cells) (n=5 wells/strain/condition). (E) Staining for mitotic marker phospho-Histone H3 (pHH3) was used to identify proliferating CFs in response to ISO. (F) Proliferation of CFbs after ISO treatment was measured by comparing the number of pHH3<sup>+</sup> nuclei relative to total nuclei (n=5 wells/strain/condition). DAPI was used to stain nuclei. Data presented as mean  $\pm$  SEM. Student t-test, \*P < 0.05. Scale bar: 200 $\mu$ m.



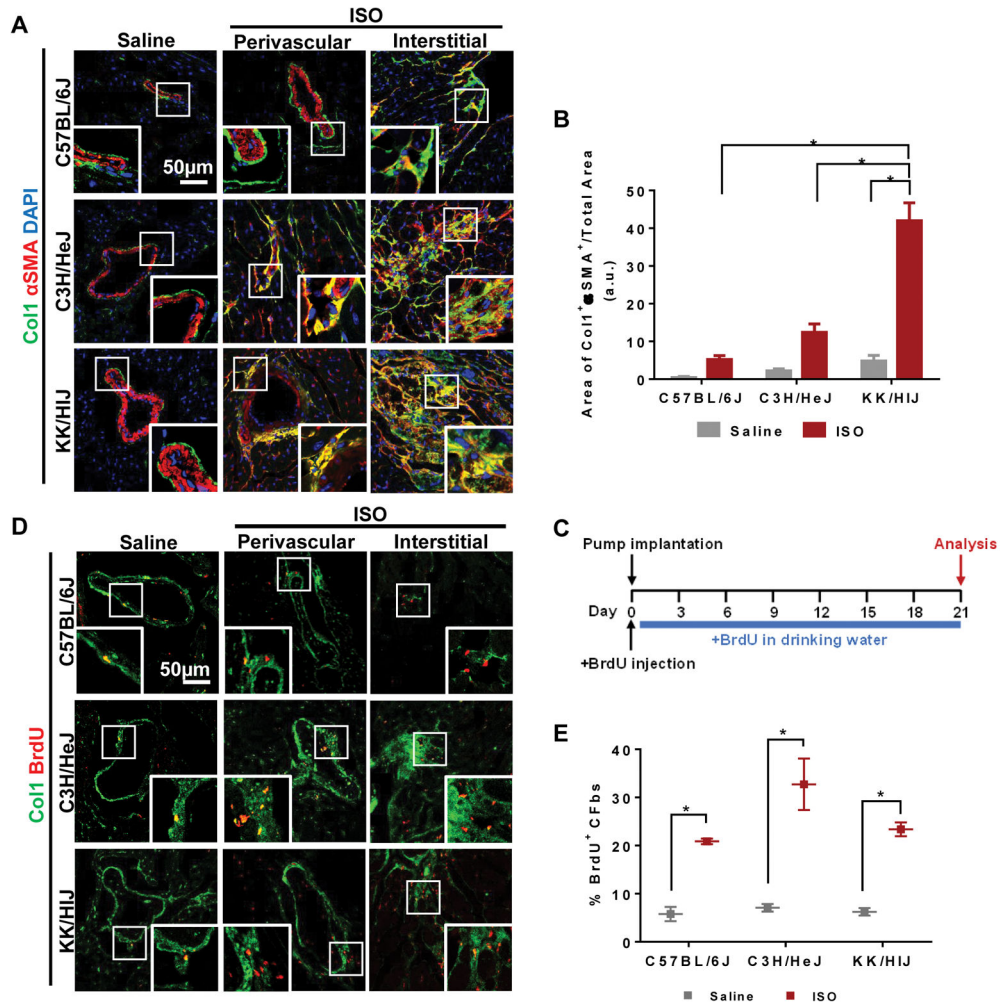


**Figure 3. CFbs display a distinct pattern of activation and proliferation that is strain-specific after *in vivo* ISO treatment**

(A) Heart sections from different strains after treatment with saline or ISO stained for  $\alpha$ SMA (red) and Col1 (green) show presence of activated fibroblasts in perivascular and interstitial fibrotic areas. (B) Quantification of Col1<sup>+</sup> $\alpha$ SMA<sup>+</sup> co-localized areas as a percentage of total heart section area (n=3–4 hearts per strain/condition). (C) Schematic of *in vivo* bromodeoxyuridine (BrdU) administration. (D) IHC of heart sections from different strains after treatment with saline or ISO shows BrdU<sup>+</sup> cells within Col1<sup>+</sup> perivascular and interstitial fibrotic regions. (E) The extent of CFb proliferation is depicted as the percentage of BrdU<sup>+</sup> CFbs within the entire Thy<sup>+</sup>HE<sup>-</sup> population in each strain after saline or ISO treatment (n=12/strain/condition). DAPI was used to stain nuclei. Data presented as mean  $\pm$  SEM. Two-way ANOVA, \*P< 0.05. Scale bar: 50 $\mu$ m

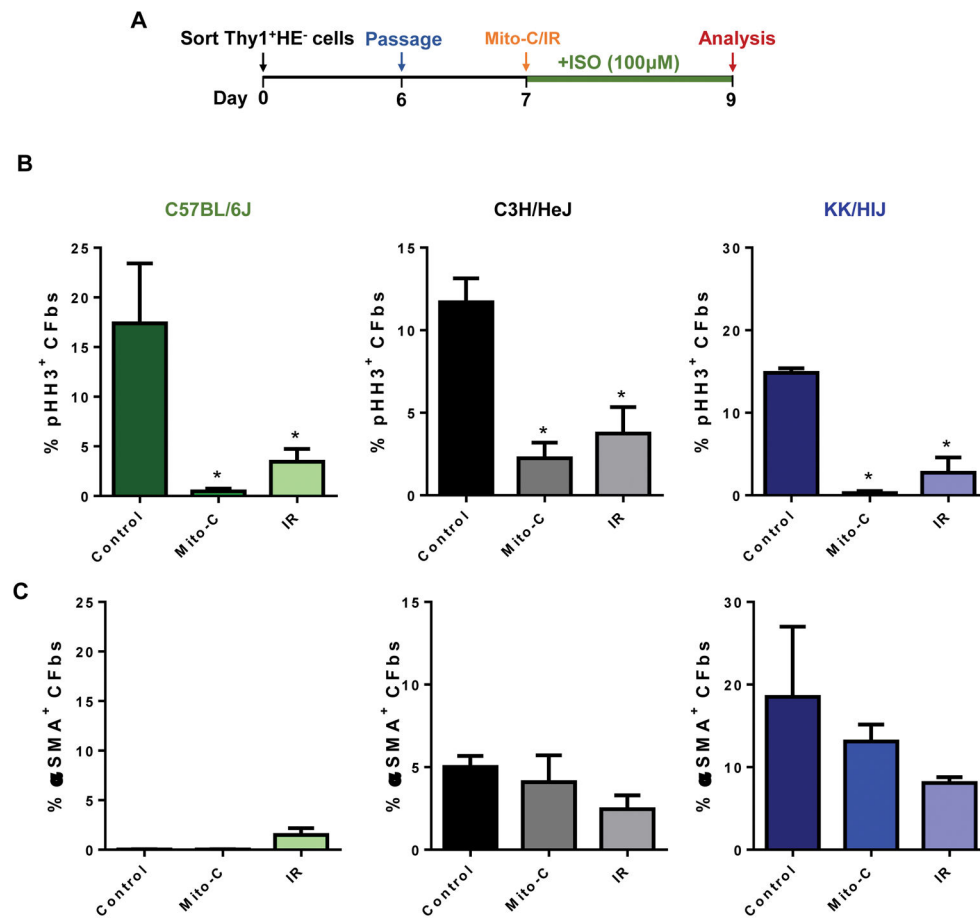


**Figure 4. Inhibiting CFb proliferation does not affect CFb activation levels *in vitro***

(A) Schematic diagram outlining the experimental design. Cells were cultured in control media, media with mitomycin-C (mito-C), or irradiated (IR) prior to ISO treatment. (B) Proliferation of CFbs after ISO treatment was measured by comparing the number of pHH3<sup>+</sup> nuclei relative to total nuclei (n=4 wells/strain/condition). (C) Activated Col1<sup>+</sup>αSMA<sup>+</sup> cells are shown as a percentage of double-positive cells relative to all Col1<sup>+</sup> cells (n=4 wells/strain/condition). Data presented as mean ± SEM. One-way ANOVA, \*P < 0.05.

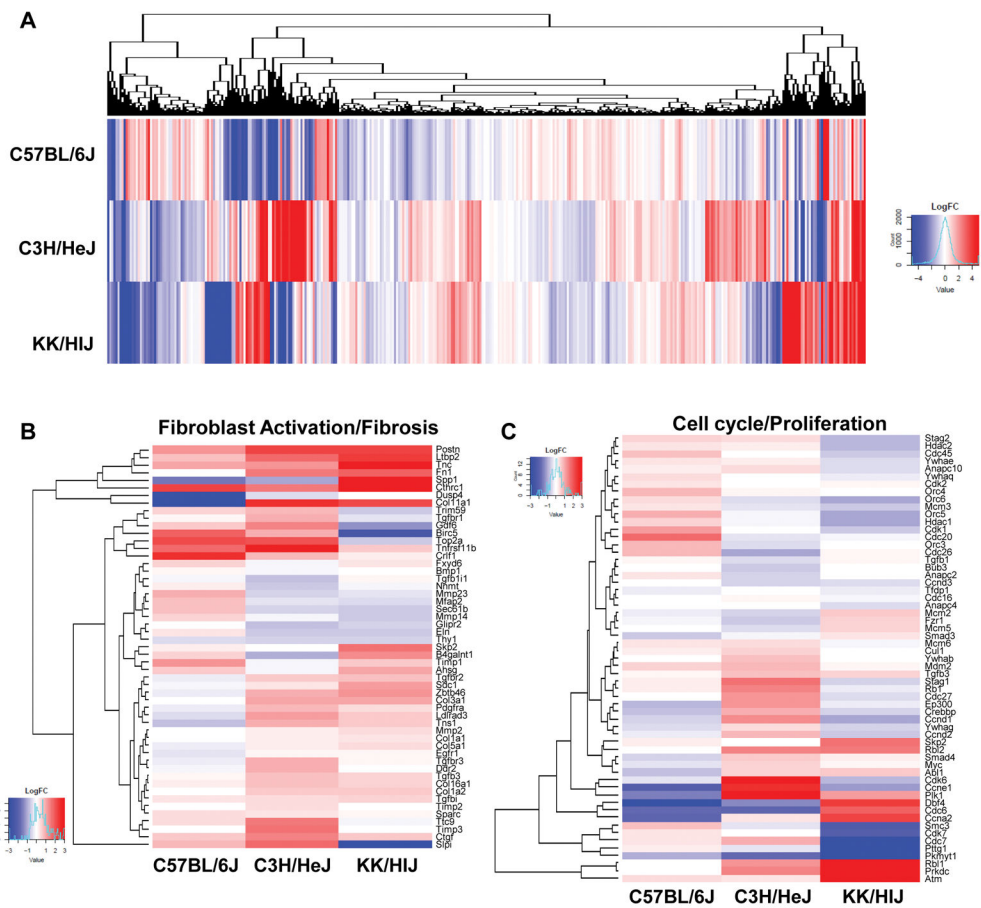


**Figure 5. ISO treatment induces unique gene expression patterns in CFbs of different strains after 21 days**  
**(A)** Heat map showing log2 fold change of differentially expressed genes in CFbs of all strains after 21 days of ISO treatment. **(B)** Heat map representing the log2 fold change value of select differentially expressed genes involved in fibroblast activation and fibrosis. **(C)** Heat map comparing expression changes of select genes involved in cell cycle and proliferation across the three strains.

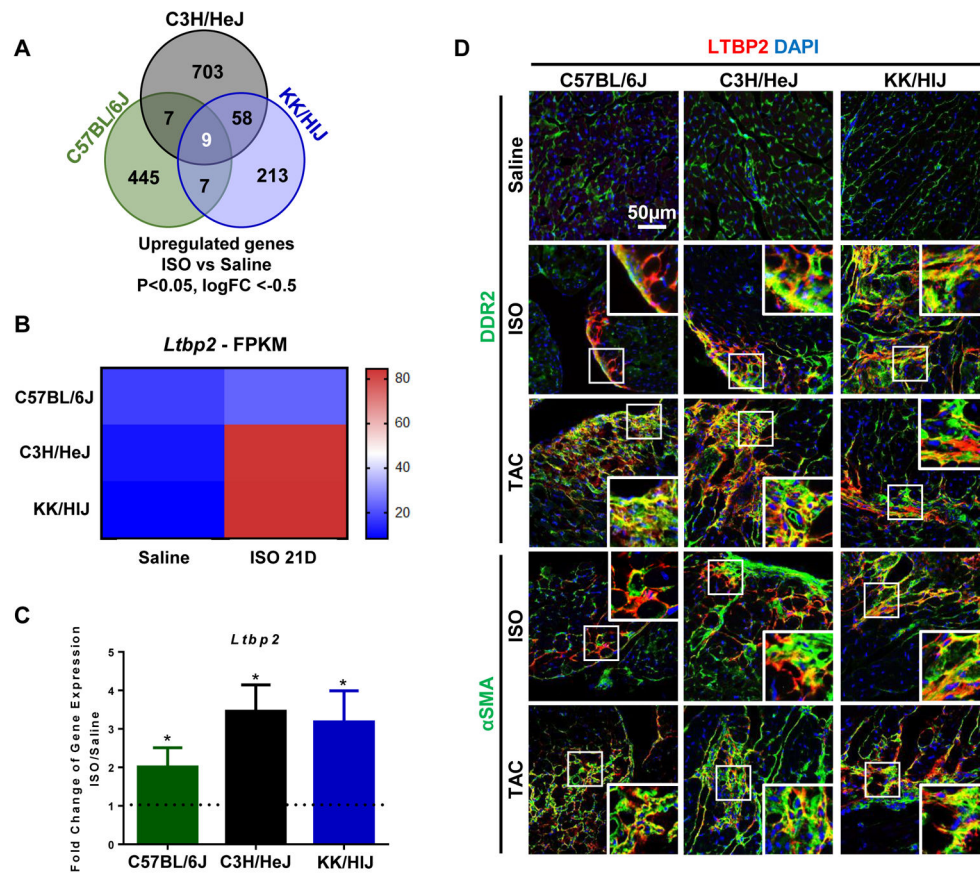


**Figure 6. *Ltbp2* is upregulated in CFbs of all strains after injury**

(A) Venn diagram depicting the number of overlapping upregulated genes across all three strains after ISO treatment. (B) Average FPKM values for *Ltbp2* in all three strains after 21 days of ISO treatment. (C) RT-qPCR analysis of *Ltbp2* after ISO treatment (n=7–9/strain/condition). (D) IHC of heart sections stained for LTBP2 (red) and DDR2 (green) or  $\alpha$ SMA (green) after ISO treatment and TAC injury. DAPI was used to stain nuclei. FPKM: fragments per kilobase of transcript per million mapped reads. TAC: transverse aortic constriction. Data presented as mean  $\pm$  SEM. Student t-test, \* $P < 0.05$ . Scale bar: 50  $\mu$ m